Solid-State NMR Study of Ibuprofen Confined in MCM-41 Material

Thierry Azaïs,*,† Corine Tourné-Péteilh,‡ Fabien Aussenac,§ Niki Baccile,† Cristina Coelho,† Jean-Marie Devoisselle,*,‡ and Florence Babonneau†

Université Pierre et Marie Curie−Paris 6, UMR 7574, Laboratoire Chimie de la Matière Condensée de Paris, Paris F-75005, France, Laboratoire de Matériaux Catalytiques et Catalyse en Chimie Organique, UMR 5618/ENSCM/Université Montpellier 1, 8 rue de l'Ecole Normale, 34296 Montpellier Cedex 5, France, and Bruker Biospin, 34 rue de l'industrie, 67166 Wissembourg, France

Received July 5, 2006. Revised Manuscript Received October 20, 2006

Ibuprofen (an anti-inflammatory drug that is a crystalline solid at ambient temperature) has been encapsulated in MCM-41 silica matrices with different pore diameters (35 and 116 Å). Its behavior has been investigated by magic angle spinning (MAS) ^{1}H, ^{13}C, and ^{29}Si solid-state NMR spectroscopy at ambient and low temperature. This study reveals an original physical state of the drug in such materials. At ambient temperature, ibuprofen is not in a solid state (crystalline or amorphous) and is extremely mobile inside the pores, with higher mobility in the largest pores (116 Å). The interaction between ibuprofen and the silica surface is weak, which favors fast drug release from this material in a simulated intestinal or gastric fluid. The quasi-liquid behavior of ibuprofen allows the use of NMR pulse sequences issued from solution-state NMR, such as the INEPT sequence, to characterize these solid-state samples. The solid-state MAS NMR study shows that the proton of the carboxylic acid group of ibuprofen is in a chemical exchange at ambient temperature. Furthermore, at low temperature (down to 223 K), NMR spectroscopy results show that ibuprofen is able to crystallize inside the largest pores (116 Å), whereas a glassy state is obtained for the smallest ones (35 Å).

Introduction

Since the last 20 years, porous silica matrices have been studied for their ability to store drugs and control drug release.[1] Recently, micelle-templated silica materials (MTS) have received considerable interest for this purpose, and nonsteroidal anti-inflammatory drugs, such as ibuprofen, have been largely used as model molecules.[2−5] Up to now, the main studies have been done with MCM-41 type materials (an MTS silica material showing a hexagonal mesoporous network with narrow pore size distribution and both large surface area and mesoporous volume) in which the drugs are encapsulated starting from solutions. The drug loading depends on the solvent used in the impregnation process,[5] the type of drug,[3] the chemical modification of the surface,[6] the mean pore diameter,[7,8] and the specific surface area.[8] The release kinetics depends on different parameters such as (i) the chemical composition of the drug,[3] (ii) the pH of the dissolution medium for ionizable drugs such as ibuprofen,[5] (iii) the pore diameter,[7] (iv) the chemical composition of the silica surface,[6] (v) the pore connectivity and its geometry, and (vi) the stability of the matrix[8] in aqueous medium.

All these studies contribute to the evaluation of the ability of MTS type materials for loading and controlled release of drugs. From a pharmaceutical point of view, it is very important to precisely characterize the physical state of a drug in the dosage form. Indeed, the polymorphism of a drug can lead to different physical and chemical properties, including color, morphology, stability, dissolution, and bioavailability,[9−11] that have to be considered with regard to regulatory aspects when developing new dosage forms.[12] Different solid-state spectroscopic techniques have been developed to characterize the active pharmaceutical ingredient, excipient, physical mixtures, and the final dosage form.[13] Among them, NMR spectroscopy has become an essential technique for the solid-state characterization of pharmaceuticals.[14,15] The technique can not only differentiate different

* To whom correspondance should be addressed. E-mail: azais@ccr.jussieu.fr (T.A); devoisse@enscm.fr (J.M.D.).
† Université Pierre et Marie Curie−Paris 6.
‡ Université Montpellier.
§ Bruker Biospin.

(1) Unger K.; Rupprecht H.; Valentin B.; Kircher W. *Drug Dev. Ind. Pharm.* **1983**, *9* (1−2), 69.
(2) Vallet-Regi, M.; Ramila, A.; del Real, R. P.; Perez-Pariente, J. *Chem. Mater.* **2001**, *13*, 308.
(3) Aiello, R.; Cavallaro, G.; Giammona, G.; Pasqua, L.; Pierro, P.; Testa, F. *Stud. Surf. Sci. Catal.* **2002**, *142*, 1165.
(4) Lai, C.-Y.; Trewyn, B. G.; Jeftinija, D. M.; Jeftinija, K.; Xu, S.; Jeftinija, S.; Lin, V. S.-Y. *J. Am. Chem. Soc.* **2003**, *125*, 4451.
(5) Charnay, C.; Begu, S.; Tourne-Peteilh, C.; Nicole, L.; Lerner, D. A.; Devoisselle, J.-M. *Eur. J. Pharm. Biopharm.* **2004**, *57*, 533.
(6) Munoz, B.; Ramila, A.; Perez-Pariente, J.; Diaz, I.; Vallet-Regi, M. *Chem. Mater.* **2003**, *15*, 500.
(7) Horcajada, P.; Ramila, A.; Perez-Pariente, J.; Vallet-Regi, M. *Microporous Mesoporous Mater.* **2004**, *68*, 105.
(8) Anderson, J.; Rosenholm, J.; Areva, S.; Linden, M. C*hem. Mater.* **2004**, *16*, 4160.
(9) Khan, G. M.; Jiabi, Z. *Drug Dev. Ind. Pharm.* **1998**, *24* (5), 463.
(10) Agrawal, S.; Ashokraj, Y.; Bharatam, P. V.; Pillai, O.; Panchagnula, R. *Eur. J. Pharm. Biopharm.* **2004**, *22*, 127.
(11) Gonzalez Novoa, G. A.; Heinämäki, J.; Mirza, S.; Antikaimen, O.; Iraizoz Colarte, A.; Suzarte Paz, A.; Yliruusi, J. *Eur. J. Pharm. Biopharm.* **2005**, *59*, 343.
(12) Raw, A. S.; Furness, M. S.; Gill, D. S.; Adams, R. C.; Holcombe, F. O.; Yu, L. X. *Adv. Drug Delivery Rev.* **2004**, *56*, 397.
(13) Bugay, D. E. *Adv. Drug Delivery Rev.* **2001**, *48*, 43.
(14) Tishmack, P. A.; Bugay, D. E.; Byrn, S. R. *J. Pharm. Sci.* **2003**, *92*, (3), 441.
(15) Saindon, P. J.; Cauchon, N. S.; Sutton, P. A.; Chang, C-J.; Peck, G. E.; Byrn, S. R. *Pharm. Res.* **1992**, *10* (2), 197.

10.1021/cm061551c CCC: $33.50
Published on Web 12/19/2006

solid-state forms of the drug but also intimately probe the structural aspects of each solid-state form.

These drug-loaded materials are supposed to have the same charcteristics as confined systems. Numerous studies have been performed on small model molecules (such as water,[16−20] methanol,[21,22] benzene,[23−27] or toluene[28−30]) confined in MCM-41[21,28,29,31] or SBA-15[21,25,27−29]. These systems were studied from ambient to low temperature by DSC (differential scanning calorimetry)[27,32], quasielastic neutron scattering,[22,28,31] or NMR spectroscopy[25−27] and revealed that the entrapment of the molecules has a direct impact on their physical properties, including the phase transition from liquid to solid. Usually, the ^{1}H, ^{2}H, or ^{13}C NMR studies were performed in a static mode with fully enriched samples (for ^{13}C and ^{2}H)[33] and consist of a line shape analysis of the signal as a function of temperature. The behavior of the molecules depends on different parameters such as the pore diameter, the nature of the matrix, the pore topology, the guest-molecule/surface[34,35] as well as the guest-molecule/guest-molecule interactions. Few studies have been done to characterize the interactions between the MTS materials and the drug.[36−40]

In this paper, we report a complete solid-state NMR study of ibuprofen (Figure 1), an anti-inflammatory drug, encapsulated in MCM-41 with two different pore diameters, 35 Å (**ibu-35**) and 116 Å (**ibu-116**). This study is essential for understanding the relationship between the nature of the interactions between the silica surface and the guest molecules and the drug release kinetics that are very fast in simulated biological fluids (gastric and intestinal).[39] Furthermore, we show that solid-state NMR spectroscopy is a powerful tool for studying the physical state of a confined bioactive substance in MTS materials. Compared to previous NMR studies on confined systems, there are two main differences in the chemical nature of the entrapped molecule: (i) first, ibuprofen is a solid at ambient temperature, when all the earlier works were reported on liquids, and (ii) ibuprofen has a relative chemical complexity when compared to previous molecules studied (water, methanol, benzene, or toluene), which have quite simple ^{1}H and ^{13}C spectra, in terms of chemical shift, that can be recorded in the static mode. Consequently, all our samples were studied under magic angle spinning (MAS) conditions to obtain high-resolution spectra. Multinuclear (^{1}H, ^{13}C, ^{29}Si) solid-state NMR experiments were used to characterize the system. Emphasis was placed on ^{1}H solid-state NMR (at ambient and low temperature) and two-dimensional correlation experiments to characterize the interactions between the guest molecules and the silica host matrix.

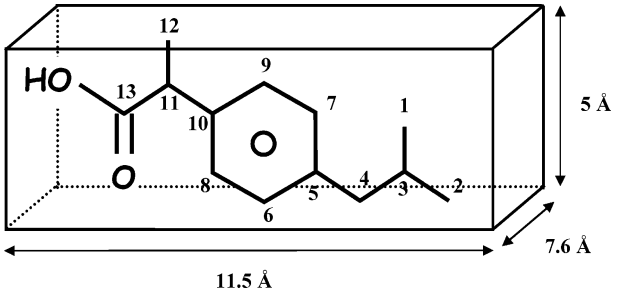

Figure 1. Schematic representation of ibuprofen with dimensions and atom labeling.

Experimental Section

MCM-41 Sample Synthesis. MCM-41 with a mean pore diameter of 35 Å was obtained by mixing H_2O, NaOH, cetyltrimethylammonium bromide, and silica (Aerosil 200), in a given molar ratio of 20:0.3:0.15:1, respectively, under magnetic stirring at room temperature. MCM-41 with a mean pore diameter of 116 Å was prepared by mixing H_2O, NaOH, cetyltrimethylammonium bromide, trimethylbenzene, and silica (Aerosil 200), with a molar ratio of 27:0.31:0.13: 0.17:1, under stirring with an inox helix at room temperature. The mixtures were then placed in a sealed inox reactor and heated at 388 K (115 °C) for 20 h.[41] The resulting white powder was washed with distilled water up to neutral pH and then dried at 323 K (50 °C) for at least 48 h for MCM-41−35 Å or one week for MCM-41−116 Å, in order to remove all the trimethylbenzene. Samples are then calcined at 883 K (610 °C) for 8 h under air flux to remove the surfactant.

MCM-41 Loading. The calcined samples are activated under a vacuum at 423 K (150 °C) for 12 h. Both samples are loaded with a solution of ibuprofen in ethanol (0.100 g cm^{-3}) according to the incipient wetness procedure previously described.[5] Briefly, this

(16) Patrick, W. A.; Kemper, W. A. *J. Phys. Chem.* **1938**, *42*, 369.
(17) Rennie, G. K.; Clifford, J. *J. Chem. Soc.* **1977**, *F1 73*, 680.
(18) Koga, K.; Gao, G. T.; Tanaka, H.; Zeng, X. C. *Nature* **2001**, *412*, 802.
(19) Moshl, R. J.; Joseph, S.; Aluru, N. R.; Jackobson, E. *Nano Lett.* **2003**, *3*, 5, 589.
(20) Tang, X.-P.; Chartkunchand, K. C.; Wu, Y. *Chem. Phys. Lett.* **2004**, *399*, 456.
(21) Morishige, K.; Kawano, K. *J. Chem. Phys.* **2000**, *112* (24), 11023.
(22) Morineau, D.; Guégan, R.; Xia, Y.; Alba-Simionesco, C. *J. Chem. Phys.* **2004**, *121* (3), 1466.
(23) Jackson, C. L.; McKenna, G. B. *J. Chem. Phys.* **1990**, *93* (12), 9002.
(24) Watanabe, A.; Iiyama, T.; Kaneko, K. *Chem. Phys. Lett.* **1999**, *305*, 71.
(25) Gedat, E.; Schreiber, A.; Albrecht, J.; Emmler, T.; Shenderovich, I.; Findenegg, G. H.; Limbach, H-H.; Buntkowsky, G. *J. Phys. Chem. B* **2002**, *106*, 1977.
(26) Aksnes, D. W.; Kimtys, L. *Solid State Nucl. Magn. Res.* **2004**, *25*, 146.
(27) Dosseh, G.; Y. Xia, C. Alba-Simionesco, *J. Phys. Chem. B* **2003**, *107*, 6445.
(28) Morineau, D.; Xia, Y.; Alba-Simionesco, C. *J. Chem. Phys.* **2002**, *117* (19), 8966.
(29) Moreno, A. J.; Colmenero, J.; Alegria, A.; Alba-Simionesco, C.; Dosseh, G.; Morineau, D.; Frick, B. *Eur. Phys. J. E* **2003**, *12*, 11.
(30) Alba-Simionesco, C.; Dosseh, G.; Dumont, E.; Frick, B.; Geil, B.; Morineau, D.; Teboul, V.; Xia, Y. *Eur. Phys. J. E* **2003**, *12*, 19.
(31) Kittaka, S.; Iwashita, T.; Serizawa, A.; Kranishi, M.; Takahara, S.; Kuroda, Y.; Mori, T.; Yamaguchi, T. *J. Phys. Chem B* **2005**, *109* (49), 23162.
(32) Jaackson, C. L.; McKenna, G. B. *Chem. Mater.* **1996**, *8*, 2128.
(33) Lusceac, S, A.; Koplin, C.; Medick, P.; Vogel, M.; Brodie-Linder, N.; LeQuellec, C.; Alba-Simionesco, C.; Roessler, E. A. *J. Phys. Chem. B* **2004**, *108* (43), 16601.
(34) Takei, T.; Konishi, T.; Fuji, M.; Watanabe, T.; Chikazawa, M. *Thermochim. Acta* **1995**, *267*, 159.
(35) Radhakrishnan, R.; Gubbins, K. E.; Sliwinska-Bartkowiak, M. *J. Chem. Phys.* **2000**, *112* (24), 11048.
(36) Ramila, A.; Munoz, B.; Perez-Pariente, J.; Vallet-Regi, M. *J. Sol−Gel Sci. Technol.* **2003**, *26*, 1199.
(37) Babonneau, F.; Camus, L.; Steunou, N.; Ramila, A.; Vallet-Regi, M. *Mater. Res. Soc. Symp. Proc.* **2003**, *778*, 3261.
(38) Babonneau, F.; Yeung, L.; Steunou, N.; Gervais, C.; Ramila, A.; Vallet-Regi, M. *J. Sol−Gel Sci. Technol.* **2004**, *31*, 219.
(39) Tourne-Peteilh, C.; Lerner, D. A.; Charnay, C.; Nicole, L.; Begu, S.; Devoisselle, J-M. *Chem. Phys. Chem* **2003**, *3*, 281
(40) Song, S-W.; Hidajat, K.; Kawi, S. *Langmuir* **2005**, *21*, 9568.
(41) Desplantier-Giscard, D.; Galarneau, A.; Di Renzo, F.; Fajula, F. In *Zeolites and mesoporous materials at the dawn of the 21st century*, Stud. Surf. Sci. Catal., 2001 (135).

process consists of four successive impregnations of 0.500 g of MCM-41 with a small amount of the solution, allowing the powder to just be wetted. The solvent is removed between two impregnations by heating at 333 K (60 °C) overnight. Samples are quickly washed with ethanol to remove the excess crystallized ibuprofen. The MCM-41−35 Å and −116 Å ibuprofen-loaded samples will be referred in the forthcoming text as **ibu-35** and **ibu-116**, respectively.

A reference sample was prepared in order to mimic the effect of thermal treatment on ibuprofen during the loading process: four successive deposits of a solution of ibuprofen (0.100 g/mL) were done in a glass flask and evaporated at 333 K (60 °C), resulting in a viscous mixture of ibuprofen and ethanol.

Characterizations of the Loaded Materials (ibu-35 and ibu-116). Thermogravimetric analysis (TGA) were carried out on a Perkin-Elmer TGA 6 balance under an air flow with a heating rate of 5 K min^{-1} up to 1073 K (800 °C). Nitrogen adsorption/desorption isotherms were recorded at 77 K (−196 °C) with a Coulter SA 3100 apparatus. Calcined samples were previously heated at 523 K (250 °C) under a vacuum overnight; loaded samples were heated at 308 K (35 °C) in order to preserve ibuprofen (heating point at 343 K). FTIR spectra in KBr pellets were obtained on a Magna-IR 550 Nicolet spectrometer.

^{1}H MAS NMR experiments were carried out on an AVANCE 300WB Bruker spectrometer (B_0 = 7.05 T) with a 4 mm probe-head and a radio frequency field ν_{1H} = 60 kHz, and on a AVANCE 400WB Bruker spectrometer (B_0 = 9.4 T) with a 2.5 mm probe and a radio frequency field ν_{1H} = 60 kHz. Samples were spun at the magic angle using ZrO_2 rotors (ν_{MAS} = 7 and 14 kHz for the 4 mm probe and ν_{MAS} = 35 kHz for the 2.5 mm probe). The recycle delays (RD) were 2 and 5 s at 7 and 9.4 T, respectively. T_2*(^{1}H) apparent transverse relaxation times were measured through spin−echo experiments (90°−τ−180°−τ−acquisition) with 15 delays between 0.5 and 5 ms using monoexponential decays at ambient temperature with a 4 mm probe (ν_{MAS} = 14 kHz and B_0 = 7.05 T)).

The ^{1}H−^{29}Si HETCOR experiments were performed on an AVANCE 300 Bruker spectrometer with a 4 mm probe (ν_{MAS} = 14 kHz) with a contact time t_{CP} = 10 ms and with TPPM ^{1}H decoupling (ν_{1H} = 60 kHz) during acquisition.

The ^{13}C NMR experiments were performed on an AVANCE 300 Bruker with a 4 mm probe. The MAS experiments (ν_{MAS} = 14 kHz) were performed with a R.F. field on the ^{13}C channel ν_{13C} = 55 kHz and a continuous ^{1}H low power decoupling (ν_{1H} = 2.5 kHz) using the waltz-16 decoupling scheme applied during acquisition and recycle delay (RD = 3 s). The CP MAS experiments were recorded with ν_{MAS} = 4.5 kHz, t_{CP} = 5 ms and with TPPM ^{1}H decoupling (ν_{1H} = 60 kHz) during acquisition. The MAS refocalised INEPT experiments was recorded with ν_{1H} = 60 kHz, ν_{13C} = 55 kHz, RD = 3 s and with TPPM ^{1}H decoupling (ν_{1H} = 60 kHz) during acquisition. The INEPT transfer delay (Δ_1 = 1.6 ms) was adjusted in order to get a reasonable compromise between all the different ^{13}C signal evolutions. The refocalization delay (Δ_2 = 1.1 ms) was set up to obtain the maximum ^{13}C in-phase signal.

No temperature regulation was used for experiments recorded at ambient temperature.

Low-temperature experiments were performed on an AVANCE 400WB Bruker spectrometer using a 4 mm DVT probe. A BCU-Xtreme accessory was used to regulate sample temperature down to 223 K (−50 °C). For lower temperature, down to 183 K (−90 °C), we used a heat exchanger to produce the cooling gas. Samples were packed into 4 mm ZrO_2 rotors and ZrO_2 caps were used because of low-temperature experiments. Temperature calibration was achieved using a lead nitrate sample ($Pb(NO_3)_2$).[42]

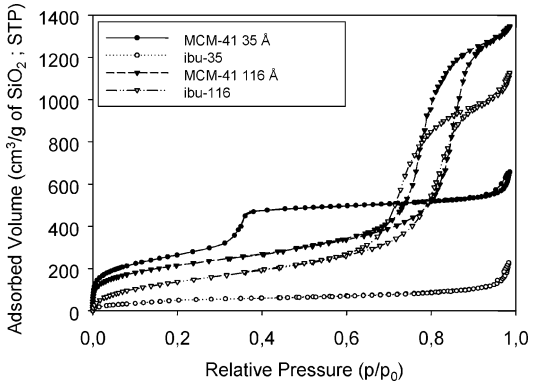

Figure 2. Nitrogen adsorption/desorption isotherms of calcinated (MCM-41−35 Å, and MCM-41−116 Å) and loaded materials (**ibu-35** and **ibu-116**). The data are normalized to 1 g of pure silica.

The chemical shift reference (0 ppm) for ^{1}H, ^{13}C, and ^{29}Si was TMS (tetramethylsilane).

Results

Porosity Characterization and TG Measurements. Nitrogen adsorption/desorption isotherms of calcined MCM-41 (35 Å and 116 Å) and loaded samples (**ibu-35** and **ibu-116**) are presented in Figure 2. Specific surface areas, evaluated by BET calculations,[43] are 987 m^2 g^{-1} and 775 m^2 g^{-1} for MCM-41−35 Å and −116 Å, respectively. The mean pore diameter is estimated by the BdB method on the desorption branch (Table 1).[44] Calcined materials exhibit type IV isotherms characteristic of mesoporosity. Nitrogen adsorption of MCM-41−35 Å does not exhibit any hysteresis loop because of truly reversible adsorption and desorption phenomena when capillary condensation occurs at p/p_0 ranging from 0.35 to 0.4. This is characteristic of MCM-41 materials with porosity about 35 Å.[45] The hysteresis loop (Type H1) of the MCM-41−116 Å isotherms is fairly narrow, with very steep and nearly parallel adsorption and desorption branches corresponding to a narrow distribution of uniform pores. The mesoporous volume is, respectively, 0.71 and 1.77 cm^3 g^{-1} for MCM-41−35 Å and −116 Å.

TG measurements (not shown) allow us to calculate the weight loss due to ibuprofen included in the inorganic matrix (Table 1). All the results are normalized to 1 g of pure silica in order to compare the different samples for a given diameter. **Ibu-35** contains 670 mg of ibuprofen per 1 g of silica and **ibu-116** contains 600 mg g^{-1}. These values are then used to correct the nitrogen adsorbed/desorbed volumes for 1 g of pure silica. Indeed, when nitrogen adsorptions are performed on loaded materials, the mesoporous volume is underestimated because the sample weight takes into account ibuprofen and pure silica. It is thus required to normalize the results to pure silica in order to compare mesoporous volumes of calcined and loaded materials.

Nitrogen isotherms of **ibu-35** are of type II, characteristic of nonporous or macroporous materials, which allows

(42) Bielecki, A.; Burum, D. P. *J. Magn. Reson.* **1995**, *116*, 215.
(43) Brunauer, S.; Emmett, P. H.; Teller, E. J. *J. Am. Chem. Soc.* **1938**, *60*, 309.
(44) Galarneau, A.; Desplantier, D.; Dutartre, R.; Di Renzo, F. *Microporous Mesoporous Mater.* **1999**, *27*, 297.
(45) Rouquerol, F.; Rouquerol, J.; Sing, K. *Adsorption by Powders and Porous Solids*; Academic Press: San Diego, 1999.

Table 1. Summary of Porosity Characteristics for Calcined (MCM-41−35 Å and MCM-41−116 Å) and Loaded Materials (ibu-35 and ibu-116)

	S_{BET} (m^2/g)	V_{meso} (cm^3/g)	isotherm type	mean pore diameter (Å)	amount of incorporated ibuprofen (mg/g)	no. of molecules (nm^2)
MCM-41−35 Å, calcined	987	0.71	IV	35		
MCM-41−35 Å, loaded (**ibu-35**)	135	0	II		670	1.98
MCM-4− 116 Å, calcined	775	1.77	IV	116		
MCM-4− 116 Å, loaded (**ibu-116**)	330	1.14	IV	96	600	2.26

Table 2. Assignments and Line Widths of ^1H and ^{13}C Signals of Ibuprofen in ibu-35 and ibu-116 Samples (corresponding to Figures 3 and 7, respectively)

site[a]		1/2	3	4[b]	5	6/7	8/9	10	11[b]	12	13
	ibu-35	0.71	1.65	2.25		6.87	7.04		3.55	1.27	
$\delta_{iso}(^1H)$		[24.3]	[39.5]	[74.8]		[26.2]	[29.0]		[31.8]	[32.5]	
[LW in Hz]	**ibu-116**	0.67	1.61	2.22		6.81	7.01		3.50	1.25	
		[22.5]	[30.2]	[44.8]		[28.2]	[27.5]		[29.8]	[30.1]	
	ibu-35	22.48	30.35	45.37	140.90	129.80	127.80	137.90	45.37	18.21	180.40
$\delta_{iso}(^{13}C)$		[30.7]	[80.6]	[138.7]	[65.2]	[107.9]	[88.2]	[62.6]	[138.7]	[48.6]	[42.4]
[LW in Hz]	**ibu-116**	21.59	30.25	45.37	140.51	129.44	127.58	137.90	45.37	17.90	180.16
		[58.8]	[84.3]	[127.9]	[60.8]	[68.5]	[84.5]	[73.5]	[127.9]	[62.8]	[45.9]
$T_2^*(^1H)$ (ms)	**ibu-35**	10.6	7.8	2.4		6.0	6.2		7.2	6.6	
	ibu-116	16.6	8.8	4.6		9.8	9.8		10.4	10.6	

[a] Labeling corresponds to Figure 1. [b] ^{13}C NMR signals from carbon 4 and 11 are overlapped.

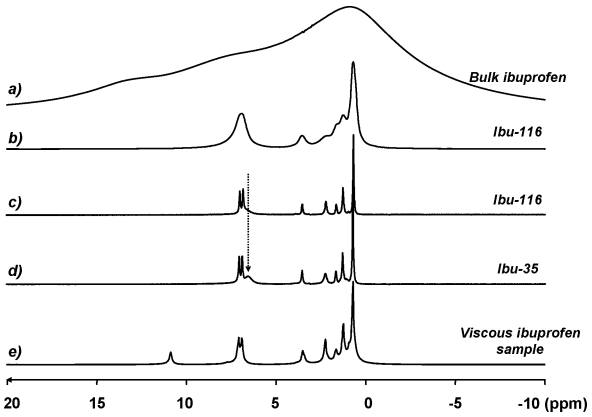

Figure 3. ^1H MAS NMR spectra of (a) crystalline ibuprofen and (b) **ibu-116** (ν_{1H} = 300 MHz; ν_{MAS} = 7 kHz) recorded at ambient temperature; ^1H MAS NMR spectra of (c) **ibu-116** and (d) **ibu-35** (ν_{1H} = 400 MHz; ν_{MAS} = 35 kHz) recorded at ambient temperature; (e) ^1H NMR spectrum of ibuprofen/ethanol recorded in static mode at ambient temperature. The arrow indicates the resonance peak at 6.7 ppm (see text for details).

unrestricted monolayer−multilayer adsorption to occur at high p/p_0 partial pressure. It indicates that the whole mesoporous network is full of ibuprofen. A weak break due to the very beginning of the pore draining, attributable to the washing step, can be seen in the isotherm slope at $p/p_0 \approx 0.22$. Moreover, Charnay and al.[5] demonstrated that this washing step allowed us to remove all the ibuprofen crystals from the MCM-41 external surface. The mesoporous volume decrease is then mainly due to the ibuprofen adsorption inside the mesopores and not to the presence of crystals that could block the pore entry. This strongly suggests that ibuprofen is mainly located inside the mesoporous network and closely packed.[5] Nitrogen isotherms of **ibu-116** keep a type IV shape with a decrease of 50% in the specific surface area, 35% in the mesoporous volume, and 20 Å in the pore mean diameter. These values indicate that ibuprofen is loaded inside the porous network, which is compatible with the size of the molecule (Figure 1). With a length of 11.5 Å, and if we consider only steric interactions, ibuprofen is able to fit in cyclindrical pores with diameters of 35 and 116 Å. Furthermore, in the case of **ibu-116**, ibuprofen does not occupy the entire mesoporous volume.

^1H Solid-State NMR Spectroscopy. Surprisingly, the ^1H MAS NMR spectra of the encapsulated ibuprofen samples, **ibu-35** and **ibu-116**, (Figure 3b, data not shown for **ibu-35**) present a very good resolution for a solid sample even at moderate MAS frequency (7 kHz). The increase of the spinning frequency up to 35 kHz leads to extremely resolved spectra (panels c and d of Figure 3). Such sharp lines (line widths between 25 and 75 Hz) are rarely observed in solid-state NMR spectra and are due to an efficient averaging of the homonuclear $^1H-^1H$ dipolar interactions coming from the reorientation of ibuprofen in the pores.[46]

For comparison, the ^1H MAS NMR spectrum of solid ibuprofen, which is a crystalline sample at ambient temperature with a melting point at 348−350 K (75−77 °C), is presented in Figure 3a. It presents broad lines characteristic of a rigid solid[47] arising from the noncomplete averaging of the strong homonuclear $^1H-^1H$ dipolar interaction. The large differences between the two NMR spectra imply that ibuprofen is not in a solid form in the pores in either a crystalline one (which is easily confirmed by X-ray diffraction experiments, not shown) or a glassy one. Ibuprofen is thus extremely mobile inside the MCM-41 host matrices at ambient temperature.

The measurements of apparent transverse relaxation times $T_2^*(^1H)$ were done through ^1H spin echo experiments using monoexponential time decay (Table 2). The rather high values compared to those of a rigid sample (from 2.4 to 16.6 ms) are consistent with the high mobility of ibuprofen in the MCM-41: the higher the mobility, the longer the $T_2^*(^1H)$ value. We can observe that these values are systematically longer for **ibu-116** compared to **ibu-35**. Ibuprofen molecules are more constrained in the smallest pores, reducing their mobility. It should also be noted that the measurements of $T_1(^1H)$ relaxation times reveal short values, still indicative of a liquidlike behavior ($T_1(^1H) \approx 1$ s).

(46) Haeberlen, U. *High Resolution NMR in Solids Selective Averaging*; Academic Press: San Diego, 1970.

(47) Azaïs, T.; Bonhomme-Coury, L.; Vaissermann, J.; Maquet, J.; Bonhomme, C. *Eur. J. Inorg. Chem.* **2002**, 2838.

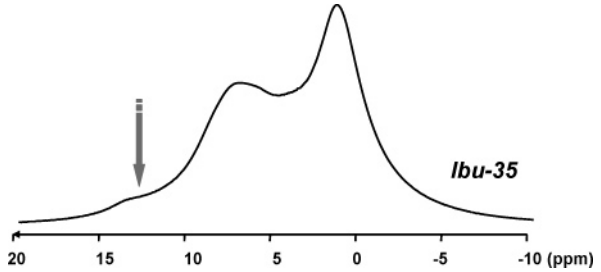

Figure 4. ^{1}H MAS NMR (ν_{1H} = 400 MHz; ν_{MAS} = 14 kHz) spectra of **ibu-35** recorded at low temperature (183 K) showing the characteristic resonance of the carboxylic proton at 13 ppm (arrow).

A viscous sample, a mixture of ethanol and ibuprofen (see Experimental Section), has been prepared in order to confirm the assumption of the "liquidlike" behavior of ibuprofen in the pores. The ^{1}H NMR spectrum of this sample, recorded in a static mode, gives a similar profile with similar chemical shifts than for **ibu-35** and **ibu-116**, confirming the resulting mobility of ibuprofen (Figure 3e).

The main regions of the ^{1}H NMR spectra can be easily assigned: peaks in the range 0−5 and 6−8 ppm are assigned to alkyl and phenyl groups, respectively, whereas the peak at 11.5 ppm is due to the proton of the carboxylic group. A complete assignment is given in Table 2 that was made using ^{1}H, ^{13}C, and ^{13}C INEPT NMR experiments performed in solution (data not shown).[38]

Surprisingly, the resonance at 11.5 ppm is absent from the spectra of **ibu-35** and **ibu-116**. A chemical exchange involving the proton of the COOH group is envisaged to explain the absence of signal. Thus, low-temperature ^{1}H MAS NMR experiments were performed from ambient temperature down to 183 K (−90 °C) on **ibu-35** (Figure 4). Resonance peaks broaden with the temperature decrease because of the reintroduction of the homonuclear ^{1}H−^{1}H dipolar couplings, with a loss of mobility. Nevertheless, using a MAS frequency of 14 kHz, resolution is sufficient to clearly observe the ^{1}H signal of the carboxylic acid group at 13 ppm. This result suggests that the carboxylic proton of the ibuprofen molecule is in chemical exchange with other protons at ambient temperature, and the most reliable hypothesis concerns the protons of the silica walls (SiOH) and/or water. Similar results have been obtained for the two encapsulated samples **ibu-35** and **ibu-116**.

To investigate the interactions involving the COOH group of ibuprofen, we performed FTIR measurements (Figure 5). The absorption band observed at 1721 cm^{-1} for crystalline ibuprofen, corresponds to the carbonyl-stretching vibration in hydrogen-bonded dimers.[48] Spectra of **ibu-35** and **ibu-116** show a shift of this band down to 1709 cm^{-1}, indicating a weakening of the C═O bond.

A broad resonance at 6.7 ppm is observed in the ^{1}H NMR spectra of **ibu-35** and **ibu-116** (arrow in panels c and d of Figure 3) that is absent from the spectrum of the viscous sample (Figure 3e). To identify the origin of this peak, we have performed cross-polarization (CP) two-dimensional heteronuclear correlation (HETCOR) experiments: magnetization is transferred from abundant nuclei (^{1}H) to non-

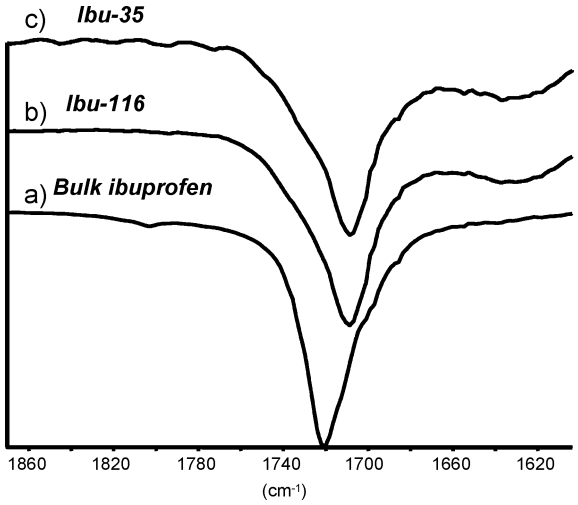

Figure 5. FTIR spectra of (a) crystalline ibuprofen, (b) **ibu-116**, and (c) **ibu-35**.

abundant ones (^{13}C and ^{29}Si) through space, i.e., via the heteronuclear ^{1}H−X dipolar interaction with X = ^{13}C or ^{29}Si. Such experiments give information about the proximity between protons and X, because the dipolar interaction depends on the inverse of the distance between ^{1}H and X nuclei.[49]

Because of the large mobility of the ibuprofen molecules that partially average the dipolar interactions, the efficiency of the cross-polarization transfer is notably reduced (when compared to a solid sample), which implies a poor signal-to-noise ratio in the ^{1}H−^{13}C HETCOR experiments. The ^{1}H−^{29}Si HETCOR experiment performed on **ibu-35** (Figure 6)

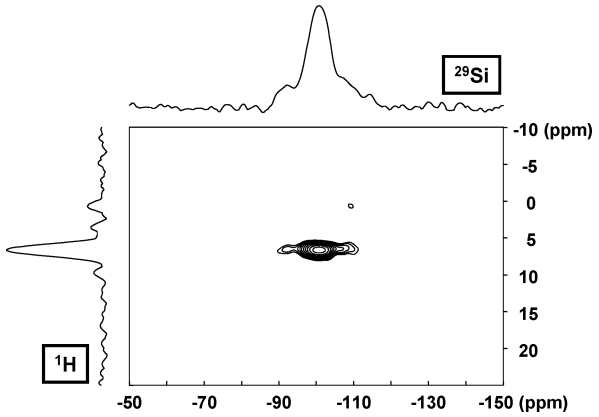

Figure 6. ^{1}H−^{29}Si HETCOR spectrum of **ibu-35** (ν_{MAS} = 14 kHz; t_{CP} = 10 ms) recorded at ambient temperature and the corresponding ^{1}H and ^{29}Si projections.

gives a clear correlation between the silicon signals from the matrix (namely Q_2, Q_3, and Q_4 signals) and the proton resonance at 6.7 ppm. On the other hand ^{1}H−^{13}C HETCOR (not shown) gives no correlation between the carbon signals from ibuprofen and the proton signal at 6.7 ppm at short (500 μs) as well as long (10 ms) contact times. This shows that the latest resonance comes from protons of the silica matrix (adsorbed water and/or silanols) and not from ibuprofen. Furthermore, the absence of any correlation

(48) Freer, A. A.; Bunyan, J. M.; Shankland, N.; Sheen, D. B. *Acta Crystallogr., Sect. C* **1993**, *49*, 1378.

(49) Schmidt-Rohr, K.; H. Spiess, W. *Multinuclear NMR in Solids and Polymers*; Academic Press: San Diego, 1996.

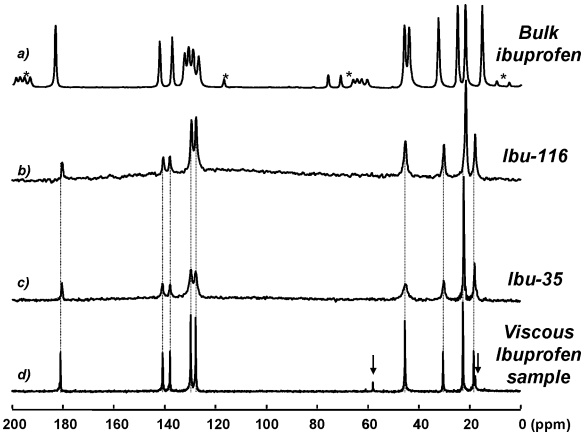

Figure 7. (a) ^{13}C CP MAS NMR spectrum of crystalline ibuprofen (ν_{MAS} = 4.5 kHz; t_{CP} = 5 ms); ^{13}C MAS spectrum of (b) **ibu-116** and (c) **ibu-35**, recorded with continuous low proton decoupling during acquisition and recycle delay (ν_{MAS} = 14 kHz; $\nu_{dec\{1H\}}$ = 2.5 kHz); and (d) ^{13}C NMR spectrum of ibuprofen/ethanol (static mode). Arrow indicates ^{13}C resonances of ethanol (* = spinning side bands).

between ibuprofen proton signals and silicon signal from the matrix is coming from the mobility of ibuprofen in MCM-41 pores.

^{13}C Solid-State NMR Spectroscopy. The ^{13}C MAS NMR spectrum of a solid sample is usually acquired using the CP (cross-polarization) technique. As previously mentioned, the efficiency of this technique in the present case is notably reduced because of the mobility of ibuprofen. In particular, the signals of the quaternary carbons are barely observed under CP conditions (not shown).

Thus, ^{13}C MAS spectra of **ibu-35** and **ibu-116** were acquired using a solution state NMR procedure (panels b and c of Figure 7). A continuous low decoupling sequence, namely waltz 16, was applied during the acquisition and the recycle delay (see Experimental Section) in order to enhance the ^{13}C signal by the nuclear overhauser effect (NOE).[50] The gain in intensity is significant when compared to a single-pulse MAS experiment (SPE), particularly for the methyl carbons (×3). The spectra obtained for **ibu-35** and **ibu-116** are similar, and a complete assignment is given in Table 2.

The ^{13}C SPE MAS NMR spectrum of the viscous ibuprofen/ethanol sample obtained in the static mode is shown in Figure 7d for comparison (quantification of the ibuprofen:ethanol molar ratio gives approximately 3:1). The spectrum is very close, in terms of number of resonance peaks and chemical shifts, to the spectra of **ibu-35** and **ibu-116**, confirming the liquidlike nature of ibuprofen in the pores. Interestingly, the ethanol signal at 58 ppm is absent from the spectra of **ibu-35** and **ibu-116**, showing the good efficiency of the drying procedure.

For the same purpose of comparison, the spectrum of crystalline ibuprofen is also given in Figure 7a. In that case, the peak positions are very different from the response of encapsulated ibuprofen, with more peaks being present in the rigid sample. In particular, the number of resonances is different in the alkyl and aromatic regions. This observation shows that there is a rapid tumbling of ibuprofen in the pores, leading to an averaging of the resonance peaks from alkyl and aromatic carbon, whereas in the crystalline solid state, the particular packing of molecules implies a crystallographic unequivalence of the various C sites.[38]

The specific mobility of ibuprofen molecules can be used to run NMR sequences taken from solution-state NMR such as refocused INEPT. This ^{1}H → ^{13}C through bond polarization transfer experiment is currently used to enhance the ^{13}C signal by ^{1}H magnetization transfer via the $^{1}J_C-H$ scalar interaction.[51] Figure 8 shows the MAS refocused INEPT pulse sequence, where Δ_1 and Δ_2 delays correspond to transfer and refocusing, respectively. Under liquid conditions, ^{13}C signals are maximized by choosing $\Delta_1 = 1/(4\ ^{1}J_C-H)$ and by adjusting Δ_2 as a function of bond multiplicities. However, in solid compounds, short T_2* values prevent us from reaching the maximum theoretical efficiency, and relaxation has to be considered. Experimentally, we found Δ_1 = 1.6 ms to be a good compromise, as $^{1}J_C-H$ values are different for aliphatic and aromatic carbons (around 125 and 155 Hz, respectively); we choose Δ_2 = 1.1 ms to get the maximum ^{13}C in-phase signal. Figure 8b shows the 1D MAS refocused INEPT {^{1}H}−^{13}C spectrum of **ibu-116**. Quaternary carbon signals are absent in the spectrum, because they are not directly bonded to a proton.

Following Alonso et al.,[52] it is possible to run 2D MAS refocused INEPT {^{1}H}−^{13}C NMR experiments in the solid state with an excellent signal-to-noise ratio. The 2D spectrum of **ibu-116** is given in Figure 8c, showing clear correlations between ^{13}C and ^{1}H signals. It allows us to establish direct C−H connectivities in the solid state and it is then very helpful in assigning the ^{13}C and ^{1}H spectrum. For example, there are clearly two different carbon sites (CH and CH_2) present under one unique signal at 45 ppm (Figure 8c).

Discussion

Entrapped molecules in silica matrices are widely studied because their physical properties are deeply modified compared to those of the bulk state. A range of small molecules have been studied, but mostly liquids at ambient temperature, such as water,[53] methanol,[21,22] toluene,[28−30] benzene,[23−27] cyclohexane,[27] and *n*-hexane.[34] These species have been entrapped in various mesoporous materials (controlled porous glasses CPG,[23,32] MCM-41,[21,28,29,31] and SBA-15[21,25,27−29]) with narrow pore size distributions (diameters of pores ∅ from 24 to 240 Å), and their behavior has been studied as a function of temperature with different techniques: DSC,[23,27,32] XRD,[21] ^{1}H, ^{2}H, or ^{13}C NMR under static conditions[25−27] and quasielastic neutron scattering (QENS).[22,28,31] These systems have also been the subject of theoretical studies.[54−56]

(50) Tozuka, Y.; Sasaoka, S.; Nagae, A.; Moribe, K.; Oguchi, T.; Yamamoto, K. *J. Colloid Interface Sci.* **2005**, *291* (2), 471.
(51) Burum, D. P.; Ernst, R. R. *J. Magn. Reson.* **1980**, *39* (1), 163. Morris, G. A.; Freeman, R. *J. Am. Chem. Soc.* **1979**, *101* (3), 760. Sorensen, O. W.; Ernst, R. R. *J. Magn. Reson.* **1983**, *51* (3), 477.
(52) Alonso,B.; Massiot, D. *J. Magn. Reson.* **2003**, *163*, 347.
(53) Grünberg, B.; Emmler, T.; Gedat, E.; Shenderovitch, I.; Findenegg, G. H.; Limbach, H-H.; Buntkowsky, G. *Chem.—Eur. J.* **2004**, *10*, 5689.
(54) Maddox, M. W.; Gubbins, K. E. *J. Chem. Phys.* **1997**, *107* (22), 9659.
(55) Radhakrishnan, R.; Gubbins, K. E.; Sliwinska-Bartkowiak, M. *J. Chem. Phys.* **2002**, *116* (3), 1147.
(56) Morineau, D.; Alba-Simionesco, C. *J. Chem. Phys.* **2003**, *118* (20), 9389.

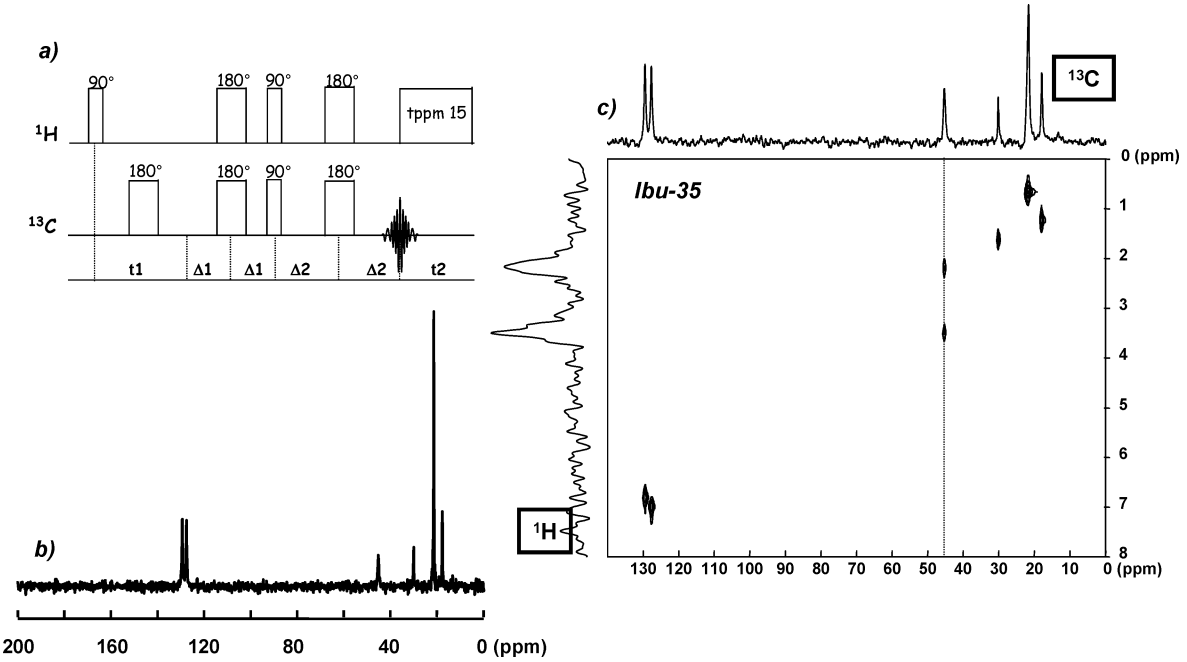

Figure 8. (a) Schematic representation of 2D MAS refocalized INEPT sequence, (b) 1D ^{13}C MAS refocalised INEPT spectrum of **ibu-116**, (c) 2D ^{1}H−^{13}C MAS refocalised INEPT spectrum of **ibu-116**. Spectrum in the ^{1}H dimension corresponds to the ^{13}C resonance at 45 ppm (ν_{MAS} = 14 kHz; Δ_1 = 1.6 ms; Δ_2 = 1.1 ms).

Authors have shown that the thermodynamic parameters of entrapped molecules greatly change when compared to those of the bulk state. For instance, the freezing or melting temperatures (T_f or T_m) are dramatically depressed. The melting point of bulk cyclohexane is 278 K. When cyclohexane is constrained in SBA-15 material with a pore diameter of 68 Å, its melting point is depressed by 73 K.[27] Furthermore, a difference between T_f and T_m is observed. Globally, observations show that the relation between the pore diameter ∅ and the difference $T_m^* - T_m$ (where T^*_m is the melting temperature for the bulk state) follows the Gibbs−Thomson equation[27]

$$\Delta T = T^*_m - T_m = [4V_m T^*_m(\gamma_{lw} - \gamma_{cw})]/[\varnothing \Delta H_m] \quad (1)$$

where V_m is the crystal molar volume, γ_{lw} and γ_{cw} are the liquid−wall and the crystal−wall interaction energies, respectively, and ΔH_m is the molar melting enthalpy. Consequently, T_m is directly related to the pore size in such a way that the narrower the pore, the lower the phase-transition temperature.

Furthermore, the crystallization of the substance at low temperature can occur only when the pore is large enough. The reason could come from the existence of a cooperative process for the nucleation, leading to a minimal critical crystal size (r_c)[32]

$$r_c = (2\sigma_{sl} T^*_m)/(\Delta H_f \rho_s \Delta T) \quad (2)$$

where σ_{sl} is the solid−liquid interfacial tension, ΔH_f is the bulk enthalpy of fusion, and ρ_s is the density of the solid. If the pore size is too small to allow nucleation, a glassy state is observed. For example, within MCM-41 with ∅ < 78 Å, authors have shown that confined methanol vitrifies on freezing.[21] On the other hand, cooling methanol confined in pores with ∅ > 90 Å results in the crystallization of the liquid. In extreme cases, a complete glass transition cannot be reached, as one can observe a mixture between molecules in a glassy state and molecules in a liquid state.[31]

Another consequence of confinement is that phase transitions (from liquid to amorphous or crystalline solid or from solid to liquid) are observed over a broad range of temperatures, unlike in the bulk state, where phase transition is a sudden phenomenon. And the more constrained the substance, the broader the temperature range. For benzene confined in SBA-15 with ∅ = 47 Å, a solidification process occurs at temperature higher than 20 K.[27]

To study the effect of confinement on ibuprofen molecules, we have recorded ^{1}H MAS NMR experiments at low temperature. This study, carefully done from ambient temperature down to 218 K in 10 K steps (Figure 9), does not show any sudden change in the proton spectrum of **ibu-35** and **ibu-116**. On the contrary, there is an homogeneous broadening of the peaks when the temperature decreases because of a progressive reintroduction of ^{1}H−^{1}H homonuclear dipolar couplings, as a consequence of the quenched mobility of ibuprofen molecules. Thus the transition from a liquidlike state to a solidlike state occurs over a broad range of temperatures, characteristic of confined species. However, we are not able to know whether the final state of ibuprofen is crystalline or amorphous because of the expected similarity between ^{1}H NMR spectra, which will be dominated by strong ^{1}H−^{1}H homonuclear couplings in both cases.

To go further, we performed low-temperature ^{13}C NMR experiments. Figure 10 displays the ^{13}C CP MAS spectra of **ibu-35** and **ibu-116** recorded at 223 K (−50 °C). The two spectra are clearly distinct. The spectrum of **ibu-116** (Figure 10a) is very different from the ^{13}C spectrum recorded at ambient temperature (Figure 7b) but close to the CP MAS spectrum of crystalline ibuprofen (Figure 7a) with identical peak positions. The spectum of **ibu-35** (Figure 10b) presents

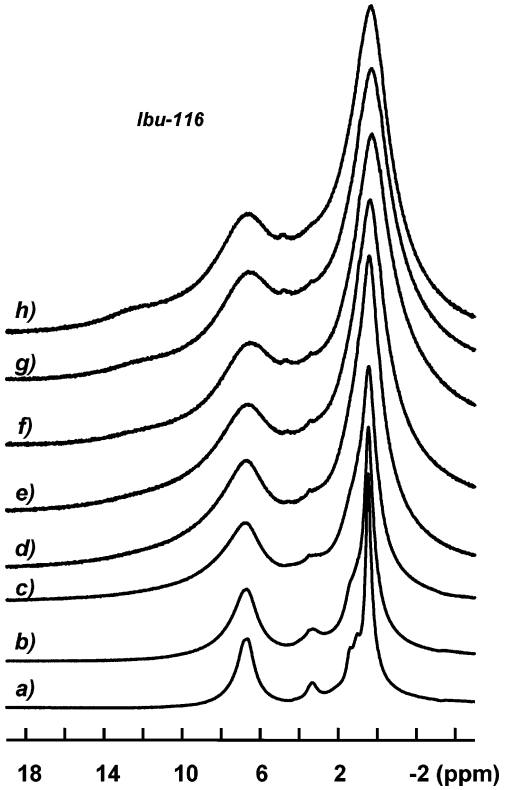

Figure 9. ^{1}H solid-state NMR MAS (ν_{1H} = 400 MHz; ν_{MAS} = 10 kHz) spectra of **ibu-116** recorded at (a) 286, (b) 276, (c) 266, (d) 256, (e) 246, (f) 236, (g) 226, and (h) 218 K.

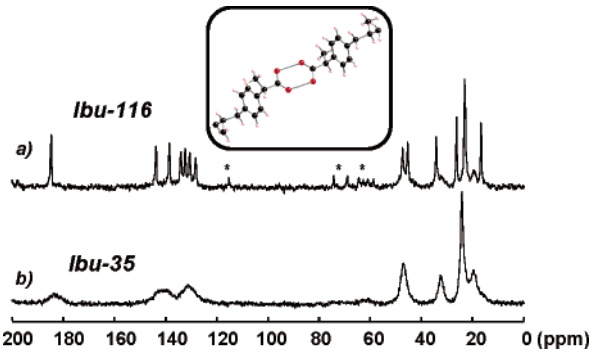

Figure 10. ^{13}C solid-state CP MAS spectra recorded at low temperature (t_{CP} = 5 ms; T = 223 K) of (a) **ibu-116** and (b) **ibu-35**. Insert shows the dimer association of ibuprofen molecules in the crystalline state. * denotes spinning side bands.

the same number of peaks with chemical shifts identical to those of the ^{13}C spectrum recorded at ambient temperature (Figure 7c) but with line widths five times larger. This leads to the conclusion that at low temperature, although ibuprofen molecules crystallize in **ibu-116**, they are quenched into a glassy state in **ibu-35.** These two radically different behaviors can be explained by steric considerations. Indeed, crystalline ibuprofen is in a dimeric form with a total length of around 26 Å.[48] Pores with diameters of 116 Å are large enough to allow the nucleation of crystallites, whereas in the small pores (35 Å), even if a dimer fits inside, this nucleation is not possible. Thus in the latter case, a vitrification process occurs, leading to a solidification of the molecules, as is proved by the increase in efficiency of the ^{13}C CP sequence. This is clearly demonstrated in the ^{13}C NMR spectrum (Figure 10b), in which the quaternary carbons are now clearly detected. It is worth noticing that at this temperature, ibuprofen in **ibu-116** is not totally under a crystalline form, as evidenced by the presence of broad peaks (at 38 and 26 ppm) in the alkyl region that correspond to a small fraction of glassy ibuprofen. Despite several attempts (slow cooling rate and long equilibration time at low temperature), it was not possible to crystallize more ibuprofen molecules in **ibu-116.** And it is worth noting that the "glassy:crystalline" ratio can vary according to the experiments.

The theoretical amount of adsorbed ibuprofen has been calculated assuming that (i) a monolayer has been formed on the entire surface and (ii) one molecule of ibuprofen occupies a mean surface value of 50 Å^2 (calculated on the basis of Langmuir adsorption experimental data, not shown). In that case, the amount of ibuprofen in the statistical monolayer corresponds to 0.675 g per g of pure silica for **ibu-35** $((987 \times 10^{20} \times 206)/(50 \times 6.02 \times 10^{23}) = 0.675$ g/g)), which is close to the adsorbed amount (0.670 g/g) determined by TG results. Using similar calculations, we found 0.530 g per g of pure silica for **ibu-116** and 0.600 g/g experimentally. According to this model, the ibuprofen monolayer entirely fills the 35 Å pores, whereas for **ibu-116**, the pore diameter decreases from 116 to 96 Å.

Similar behaviors were observed by Leto et al.[57] by means of DSC for ibuprofen confined in mesoporous silicon, and not silica. The confinement effects were not as dramatic as those detected in this study. For example, the liquid−solid phase-transition temperature is observed at 53 °C by Letho et al., whereas it is estimated to be around −50 °C in this study (the melting point of bulk ibuprofen is 75−77 °C). These data show that there are numerous parameters that influence the behaviors of confined molecules, such as the pore diameter, the topology of the porous network, the nature of the matrix interface, and the nature of the entrapped molecules, leading to different liquid−wall and solid−wall interactions. However, the way these parameters influence the molecule behavior is still not well-understood.

In this work, no hypothesis is done on the nature of the molecular diffusion of ibuprofen in the pores, which is part of another study. Nevertheless, it is worth noting that the mobility has no influence on the shelftime of such materials as soon as they are stored at 5 °C. After 1 year, no recrystallization process was observed via XRD and NMR.

In the future, particular efforts will be focused on the low-temperature NMR experiments. If we consider that freezed confined ibuprofen at 223 K is a snap shot of the system of ibuprofen molecules at ambient temperature, NMR correlation experiments via dipolar interactions between ^{1}H and ^{13}C or ^{1}H and ^{29}Si or recoupling dipolar ^{13}C−^{13}C or ^{1}H−^{1}H experiments should reveal the organization of the drug molecules in the pores and their interaction with the silica matrix.

Conclusions

In this paper, we have shown by using solid-state NMR spectroscopy that ibuprofen molecules entrapped in MCM-41 with two different pore diameters ∅ = 35 Å and ∅ =

(57) Lehto, V. P.; Vähä-Heikkilä, K.; Paski, J.; Salonen, J. *J. Therm. Anal. Calorim.* **2005**, *80*, 393.

116 Å) are extremely mobile at ambient temperature. The $^1H-^{13}C$ and $^1H-^{29}Si$ HETCOR experiments prove that there is a weak interaction between the drug and the silica matrix, which is surprising, considering the presence of a carboxylic acid group in the ibuprofen molecule that, intuitively, was supposed to interact strongly with the silica surface. The encapsulated molecules have the same behavior as a confined liquid at ambient temperature, even if its bulk nature is a rigid solid. $T_2^*(^1H)$ NMR measurements, which are longer in **ibu-116** than in **ibu-35**, show that the mobility is greater in large pores, as expected intuitively. If the two systems have the same behavior at ambient temperature, their NMR response are very different at low temperature ($T = 223$ K): ibuprofen crystallizes in **ibu-116**, whereas a vitrification of the molecules happens in the smallest pores (**ibu-35**) that is justified by steric considerations.

We exploited this mobility at ambient temperature by setting up $^1H-^{13}C$ INEPT experiments and proved that they are well-adapted to the characterization of the mobile part of such hybrid systems.

The materials were studied in the dried, state which is different from the one under in vitro drug-release conditions. Thus, the NMR results cannot directly explain the fast kinetics observed in simulated gastrointestinal fluids.[5] Nevertheless, one can affirm that the mobility associated with a noncondensed state and the weak interaction of ibuprofen with the matrix seem to favor a particularly high release rate, as ibuprofen is not tightly bonded to the matrix.

The liquidlike behavior of ibuprofen confined in MCM-41 corresponds to an original physical state of the drug in MCM-41 materials that can be related to a solid molecular dispersion.[58,59] Moreover, the drug's physical form should be controlled by the MCM-41 tunable porosity because of the confinement effect. This particular property should be of interest in order to increase the dissolution rate of poorly soluble drugs.

Acknowledgment. Jocelyne Maquet from LCMCP is warmly thanked for technical assistance. Dr. Marie-Noëlle Rager from ENSCP is greatly acknowledged for fruitful discussions. Mobility grants have been received from FAME European Network of Excellence (FP6).

CM061551C

(58) Craig, D. Q. M. *Int. J. Pharm.* **2002**, *231*, 131.
(59) Leuner, C.; Dressman, J. *Eur. J. Pharm. Biopharm.* **2000**, *50*, 47.